BMC Cancer

RESEARCH

Open Access

Dual Cas12a and multiplex crRNA CRISPR strategy ultrasensitive detection novel circRNA biomarker for the diagnosis of ovarian cancer

Lingxi Tian[1], Yan Gao[2*], Lihan Zi[1], Ruilian Zhe[3] and Jun Yang[1*]

Abstract

Background Ovarian cancer (OC), as a malignant tumor, currently lacks effective screening early diagnosis measures. Clinical biomarkers CA-125 and HE4 are limited by false positives and insufficient sensitivity. Therefore, it's of great significance to search for new biomarker and construct sensitive detection method.

Methods We found a novel circRNA biomarker (hsa_circ_0049101) by RNA sequencing, and simultaneously propose a strategy, which integrates reverse transcription rolling circle amplification (RT-RCA) and clustered regularly interspaced short palindromic repeats (CRISPR)-Cas12a to amplify and detect novel circRNA biomarker. This strategy use Dual Cas12a protein (FnCas12a and LbCas12a) and Multiplex CrRNA (DCMC-CRISPR) to enhance detection sensitivity. The sensitivity mechanism of CRISPR to detect circRNA was verified in detail.

Results The DCMC-CRISPR assay exhibited a broad detection range of 2000 pM to 0.5 fM and the limit of detection (LOD) as low as 0.5 fM. The DCMC-CRISPR system has 4–11 times higher sensitivity than single-crRNA CRISPR/Cas12a system. Clinical assessment of RNA extracts from patient's peripheral blood of 22 clinical OC patients and 28 controls demonstrates the DCMC-CRISPR strategy outperformed CA-125, HE4, and the ROMA index. The assay demonstrated comparable performance to RT-qPCR, exhibiting favorable sensitivity and specificity in this pilot cohort.

Conclusions The DCMC-CRISPR platform offers a promising solution for circRNA biomarker screening and circRNA diagnostic. It highlights the possibility of expanding its applicability to address other cancer diseases.

Keywords Ovarian cancer, CircRNA biomarker, Dual Cas12a Multiplex crRNA, CRISPR/Cas12a, Early diagnostic

Introduction

Ovarian cancer (OC) has the highest mortality rate among gynecological malignancies, and it is characterized by an insidious onset at early stages [1, 2]. Approximately 70% of patients with OC are diagnosed in the advanced stage [3]. The 5-year survival rate is only 25% for patients with advanced OC but over 85% for patients with early OC [4]. Therefore, an early diagnosis of OC is expected to effectively reduce the high mortality of this malignancy.

Serological tumor marker screening is the non-invasive early screening method in clinical practice [5, 6]. CA125 (Carcinoma Antigen 125) and HE4 (Human Epididymis Protein 4) are the most valuable tumor protein markers.

*Correspondence:
Yan Gao
lnzl123@sina.com
Jun Yang
junyang@dlut.edu.cn
[1] MOE Key Laboratory of Intelligent Biomanufacturing, School of Bioengineering, Dalian University of Technology, Dalian 116024, People's Republic of China
[2] Liaoning Cancer Hospital & Institute, Shenyang 110000, People's Republic of China
[3] Shenzhen People's Hospital, Shenzhen 518001, People's Republic of China

A higher serum level of CA125 is detected in about 90% of patients with advanced OC [7]. However, the effectiveness of this tumor protein marker is limited due to a low positive rate in the diagnosis of OC at stage I and inadequate tissue specificity [8, 9]. HE4 has shown better performance in the diagnosis of OC at an early stage. HE4 may have no abnormal levels in some patients with OC, but it has a high positive rate in the detection of endometrial cancer [10, 11]. The risk of ovarian malignancy algorithm (ROMA) index is a risk prediction model combined with the serum concentration of HE4 and CA125 and the menstrual status of patients [12, 13]. It has been demonstrated that the accuracy and sensitivity of ROMA index are higher than those of HE4 or CA125 alone. However, the sensitivity and specificity of these protein biomarkers remain limited to a certain extent compared with nucleic acid biomarkers.

Circular RNA (circRNA) is a novel class of non-coding RNA with a covalently closed configuration but without 5' end caps and 3' end poly (A) structure [14–16]. The closed loop structure of circRNA leads to a longer half-life and resistance to RNase R, contributing to its stable existence in the plasma and serum [17, 18]. CircRNAs are differentially expressed in tumors, suggesting their potential as a liquid biopsy marker for the diagnosis of diseases in humans. Their diagnostic role in OC has been confirmed in several studies. Wu et al. [19] analyzed the RNA sequencing results of tumor tissues and normal tissues of patients with OC, and they found that circFBXO7 was significantly down-regulated, which can be used as a target for the diagnosis, treatment, and prognosis of OC. Gan et al. [20] verified that circMUC16 (hsa_circ_0049116) was up-regulated in epithelial tissues in OC and it was associated with the stage of epithelial ovarian cancer (EOC) and a higher serum CA125 level. However, compared with protein biomarkers, circRNAs still have a low level in blood with difficulties in detection and quantification, which significantly impaired the sensitivity of circRNA detection is still greatly limited.

The conventional reverse transcription-quantitative polymerase chain reaction (RT-qPCR) is considered the gold standard for detecting circRNAs, but this method is limited by its low operational sensitivity and complex procedures [21]. To overcome such limitations, increaseing the quantity of the target DNA substrate by nucleic-acid amplification in advance has become the standard strategy. The amplification methods include isothermal amplification, such as loop-mediated amplification (LAMP) and rolling circle amplification (RCA) [22, 23]. Although pre-amplification can improve the sensitivity by 10^7-fold, the detection limit of amplification alone is only as low as pM.

As an RNA-guided DNase, the clustered regularly interspaced short palindromic repeat (CRISPR)/CRISPR-associated protein 12a (CRISPR/Cas12a) demonstrates a ssDNase ability (also called a collateral effect) when the Cas12a/crRNA complex is activated by the target dsDNA/ssDNA. Cas12a can be activated even at room temperature and has low mismatch tolerance [24, 25]. These characteristics enable the CRISPR/Cas12a system to be an efficient and programmable detection platform [26]. Li et al. [27] proposed a CRISPR/Cas12a strategy to sensitively detect the esophageal cancer biomarker miRNA-21. Lu et al. [28] also reported a CRISPR/Cas12a-based fluorescence bioassay combined with the strand displacement reaction (SDR) detection exosome miR-21 derived from lung cancer. Based on the biosensing technology of CRISPR, Cas nuclease can identify target genes by cleaving the crRNA complementary to the target and the short sequence protospacer adjacent motif (PAM) flanking the target. Currently, a single Cas protein and a single crRNA are mostly used in the reported CRISPR detection methods [29]. Hence, crRNAs are strictly limited by PAM site in design, and the flexibility of PAM sequences greatly limits the range of Cas nucleases that can be targeted, thus reducing the detection sensitivity.

Therefore, to improve the diagnostic accuracy and sensitivity of early OC, a highly effective novel circRNA biomarker and conceived reverse transcription rolling circle amplification (RT-RCA) pre-amplification target, designed Dual Cas12a protein Multiplex CrRNA-CRISPR system (herein after referred to as "DCMC-CRISPR"), was proposed in this study to achieve the highly specific and ultrasensitive quantitative detection of circRNA biomarkers, thus realizing the accurate diagnosis of OC (Scheme 1). Besides, database information mining was employed to statistically analyze existing circRNAs associated with the MUC16 gene. Meanwhile, circRNA sequencing (circRNA-Seq) and a series of bioinformatics analyses were performed on OC-related and normal cell lines. Consequently, a sensitive and effective circRNA (has_circ_0049101, circMUC16) were screened, and the specificity and expression of the circMUC16 in different gynecological cancer cell lines were verified using RT-qPCR. In addition, circMUC16 was quantitatively analyzed and validated in clinical blood samples using the DCMC-CRISPR strategy. Moreover, RNA extraction was conducted after clinical blood samples were collected, and RT-RCA isothermal pre-amplification was performed on the target circRNA. Specifically, a specific primer was designed at the back splice site (BSJ) of the circRNA to recognize the target. This unique cDNA was generated by RT-RCA and used as a target for subsequent CRISPR/Cas12a. Next, LbCas12a and FnCas12a were combined with four of their corresponding crRNAs

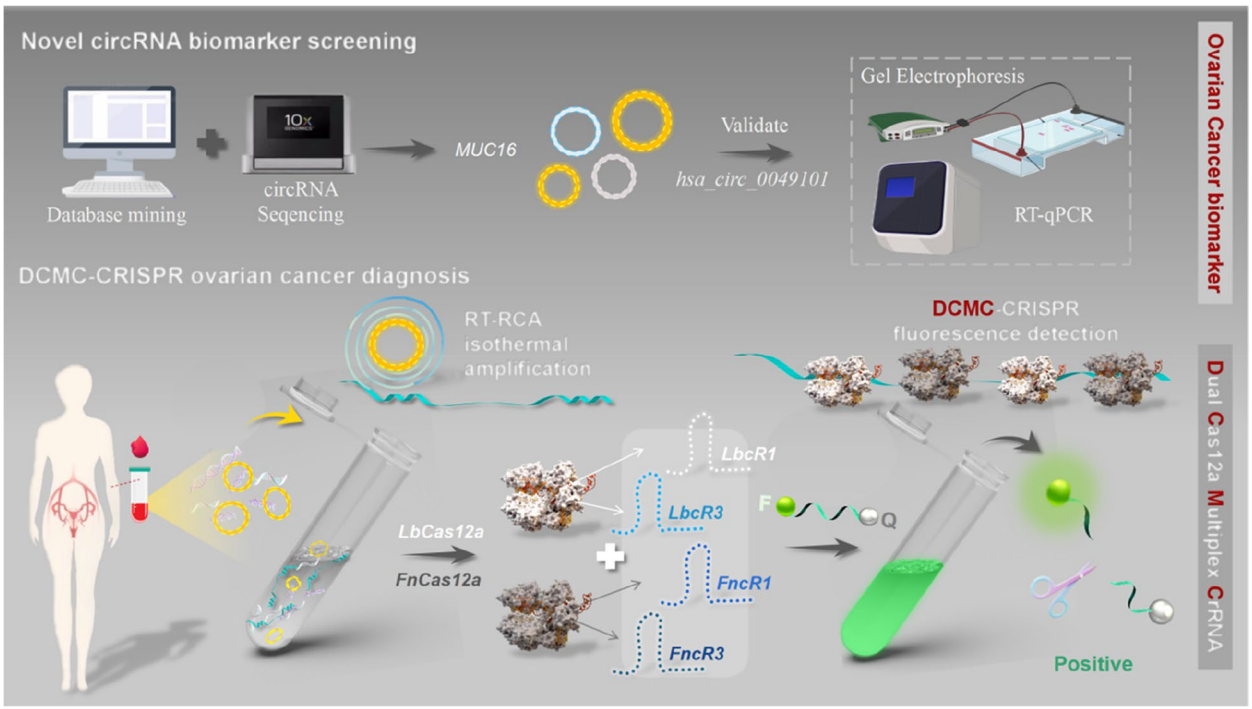

Scheme 1 Schematic illustration of novel circRNA biomarker screening and the DCMC-CRISPR strategy detection circRNA for ovarian cancer diagnosis

and then the RT-RCA amplicon (cDNA) was dynamically diffused into the CRISPR detection system. When the cDNA sequence was specifically recognized by Cas12a/crRNA complexes, The trans-cleavage of ssDNA reporters was triggered to produce a strong fluorescent signal. The combination of two Cas12a protein and multiple crRNAs resulted in the continuous activation of Cas12a protein, which further improved the detection sensitivity, thus achieving the efficient detection of target nucleic acids. Through the detection of fluorescent signals, the quantitative detection of circRNAs can be realized with higher sensitivity and specificity.

Materials and methods

Chemicals and materials

All HPLC-purified oligonucleotide sequences were presented in supplementary material Table S1 and synthesized by GenScript and TaKaRa Biological Technology Co. Ltd. (NanJing, China) with purity above 90%. T4 RNA Ligase 2, DNase I, Monarch® RNA Cleanup Kit, ProtoScript® II Reverse Transcriptase and EnGen® LbaCas12a (Cpf1) were purchased from New England Biolabs. FnCas12a was purchased from Shanghai Huicheng Company. GoScript™ Reverse Transcription System was purchased from Promega Biotech Co. Ltd. (Beijing, China). dNTP and RNase R were purchased from Beyotime Biotechnology Co. Ltd. (Shanghai, China). Gynecological cancer cell lines: ovarian cancer (NIH:OVCAR-3, SKOV3), endometrial cancer (RL-952), breast cancer (MCF-7), Cervical cancer (Hela) and normal cell 293 T were purchased from the The Cell Bank of the Chinese Academy of Sciences (Shanghai, China) and Baihao Biotechnology Co. Ltd. (Liaoning, China) were authenticated before use. Human CA125 (Carbohydrate Antigen 125) ELISA Kit and Human HE4 (epididymal protein 4) ELISA Kit were purchased from Sangon Biotech. Co., Ltd. (Shanghai, China).

circRNA biomarker data mining

Download circRNAs derived from MUC16 gene in circbase and circNET database, and statistical analysis of circRNA exons using the "ggpubr", "tidyverse" and "magrittr" package in R language. Ovarian cancer cell (NIH:OVCAR3 and SKOV3) and normal cell (293 T) total RNA were prepared for library preparation by using the Illumina Stranded Total RNA Prep. Following size exclusion and quality assessment, the sequencing libraries were pooled, and paired-end sequencing was performed using an Illumina NovaSeq platform. Next, the find_circ was used to align circRNA sequences (against homo sapiens GRCh38) and quantify circRNA expression. The circRNA abundance was calculated based on counts per million. The R package "limma" was used to perform differential expression analysis to identify

miRNA candidates between OC and controls. The circRNA-miRNA-mRNA interaction network was constructed using Cyoscape software.

Circularization of linear RNA using T4 RNA ligase 2

Linear RNA templates were in vitro transcribed by synthetic double-stranded linear DNA templates. Linear RNA was circularized using T4 RNA ligase 2 on a DNA ligation primer. After annealing with a ligation primer (5 μM), linear RNA (1 μM) was incubated in a mixture at 65°C for 5 min, cooled to 12°C at 1°C/min. with T4 RNA ligase 2 and RNase inhibitor incubated at 37°C for 90 min, then 80°C for 5 min. Subsequently, RNase R and buffer 37°C were added for 30 min and 70°C for 10 min. Excess DNA ligation primer was digested with DNase I for 30 min. The products were purified by Monarch® RNA Cleanup Kit.

CrRNA in vitro transcription

The as prepared dsDNA was used as the template to transcribe crRNA using T7 in vitro transcription kit (HiScribe™ T7 High Yield RNA Synthesis Kit) according to the manufacturer's protocol. The mixture was incubated at 37°C overnight, keep warm at 70°C for 10 min. The produced crRNA (LbcrRNA1-3, FncrRNA1-3) was purified by RNA clean Kit (NEB Monarch RNA Cleanup Kit) according to the manufacture's instruction and quantified by NanoDrop and 1.0% agarose gel electrophoresis, the gel was run at 180 V for 20 min.

The DCMC-CRISPR assay

Protoscript II Reverse Transcriptase Kit (NEB, Beijing, China) was used for RT-RCA. According to the instructions in the manual, the reagents were mixed in a PCR tube. Template for the circRNA prepared as described above in 2.3, 480 nM RT-RCA primer, Protoscript II Reverse Transcriptase, 10×DTT, 600 nM dNTP and RNase Inhibitor, The mixture was incubated at 42°C for 1 h and then heated to 65°C for 20 min. Subsequently, CRISPR/Cas12a was performed, LbcrRNA1, LbcrRNA3, FncrRNA1 and FncrRNA3 at 100 nM each, 200 nM LbCas12a, 200 nM FnCas12a, 400 nM FQ, and 10 mM DTT were added to the PCR tube. The reaction mixture was incubated at 37°C for 2 h, and the fluorescence emission spectrum was detected on an Infinite® 200 PRO microplate reader (Tecan, Switzerland). The fluorescence dynamics was performed on Quant Studio3 RealTime System (Thermo Fisher Scientific, Waltham, MA).

Statistical analysis

Receiver operating characteristic curve (ROC) was analyzed by SPSS software. ROC analysis is used to measure the predictive power of different assays for biomarkers in tumor samples. The ROC curve describes the sensitivity and specificity. AUC is usually used to measure the predictive ability of a biomarker for non-response; it ranges from 0 to 1. The higher the AUC value, the better the predictive ability. An AUC of 1.0 represents a perfect prediction. Graphics are prepared using SPSS 25.0. All quantitative data were calculated by the mean ± SD of at least three independent experiments. Two-tailed Student's t-test was used to evaluate statistical differences between two groups with a P-value < 0.05 considered to be statistically significant.

Characterization of circRNAs in clinical blood samples

Blood samples from 22 OC patients and 28 healthy donors were provided by the Liaoning Cancer Hospital & Institute (Shenyang, Liaoning, China). All recruited samples were aged 20–75 years and none had all patients were diagnosed with OC based on pathological examination and did not receive any preoperative anticancer treatment. All OC cases were confirmed by clinical pathology. In addition, informed consents were obtained from all participating subjects. Detailed clinical information including pathological types, TNM stages, age and gender on ovarian cancer patients and healthy volunteers was shown in Table S2.

RT-qPCR and the established DCMC-CRISPR assay were used to detect circRNA in the clinical samples. To conduct RT-PCR, we isolated RNA from blood samples using the miRNeasy Micro kit (Qiagen, Germany). This extraction yielded approximately 1 μg of RNA in a 20 μL solution. Next, we performed reverse transcription using the Go script reverse transcription kit. Then combined 0.4 μL of a 10 μM forward primer, 0.4 μL of a 10 μM reverse primer, 6 μL of the reverse transcribed solution, and 10 μL of qPCR SYBR Green Master Mix for the PCR reaction. The PCR process consisted of an initial predenaturation step at 95°C for 10 min, followed by 40 cycles of denaturation at 95°C for 15 s, annealing at 60°C for 60 s, and extension at 72°C for 20 s. Finally, we analyzed the PCR amplification curve and Cq value to assess the quantity of circRNA in the clinical samples. For the DCMC-CRISPR assay system, RT-RCA primer (480 nM), Protoscript II Reverse Transcriptase (400 nM), 10×DTT and dNTP (400 nM) were mixed with RNA samples and incubated at 42°C for 60 min. Next, 2 μL Cas12a protein (400 nM), 1 μL crRNA (400 nM) and 1 μL ssDNA (600 nM) were added. The mixture was incubated at 37°C for 40 min and measured using the Quant Studio 3 RealTime System.

ELISA experiment

The levels of CA125 and HE4 in the blood samples were detected by enzyme-linked immunosorbent assay

(ELISA) method, using the corresponding ELISA kits, and strictly following the instructions in the accompanying manual. 5 μL of fasting venous blood was collected from the patients in the morning, and centrifuged at 3000 rpm for 10 min to separate the serum. The serum was then divided into sterile EP tubes and stored at -80℃ in a refrigerator. The enzyme-labeled wells were pre-coated with anti-CA125 antibody or anti-HE4 antibody. 50 μL of standard and serum samples were then added to the wells and incubated at 37℃ for 1 h. The wells were then washed, and 50 μL of freshly diluted biotin-conjugated anti-CA125 or anti-HE4 antibody were added. The wells were incubated at 37℃ for 1 h and then washed again. 50 μL of color development reagent were then added, which reacted with the horseradish peroxidase-conjugated streptavidin, and incubated at 37℃ for another 30 min. The unbound enzyme was then removed by washing, 50 μL of TMB substrate were added to develop the color. Finally, the absorbance (OD) value of the reaction wells was measured at 450 nm using an ELISA reader.

Results

circMUC16 is a potential biomarker of ovarian cancer

As the largest transmembrane mucin, MUC16 (also known as CA125) is over-expressed on the surface of OC cells and sheds into the blood. Therefore, MUC16 can be used as a serum biomarker for OC [30].

The MUC16 gene contains 90 exons and exhibits a rich repertoire of alternative splicing sites. In this study, the exons of pre-existing circRNA in the database and the exons at the splicing sites of these circRNAs were statistically analyzed with the aid of the R package. The results revealed that exon 68 had a particularly high occurrence frequency at the back-splice junction (BSJ) site, demonstrating that exon 68 can be used as a potential detection target (Fig. 1A). Simultaneously, circRNA-Seq was performed on OC cells, and the potential circRNA-miRNA-mRNA regulatory network was analyzed, which yielded four potential up-regulated circRNAs (Fig. S1). Among them, has_circ_0049101 (hereafter referred to as circMUC16) consisted of three exons 66–67-68 (Fig. 1B), with up-regulated expression in OC. Besides, circMUC16 can serve as a miRNA adsorption sponge, and constitute a regulatory network with mRNA, and it was closely related to the proliferation and migration of epithelial cells (Fig. 1C, D). The database mining and sequencing analysis results corroborated that circMUC16 can be used as a potential biomarker of OC.

Next, the expression of circMUC16 in different gynecological cell lines was validated. The RNA extracted from different cell lines was reversely transcribed and circRNA detection was performed using PCR and RT-qPCR. It was found that circMUC16 was highly expressed in the OC cell lines, and NIH:OVCAR3 showed higher expression than SKOV3. However, the expression of RL-952 was detected, neither in the breast cancer cell MCF-7 nor the cervical cancer cell Hela (Fig. 1E, F). This indicated the specific expression of circMUC16 in OC cells and its potential as a diagnosis target. In 3.7, circMUC16 was further detected by RT-qPCR and DCMC-CRISPR in clinical blood samples.

Validation of the amplification system

To analyze the circRNA detection performance of DCMC-CRISPR, the circRNA (circMUC16) was designed and synthesized by in vitro transcription and RNA cyclization. The specific process of circRNA synthesis is shown in "Circularization of linear RNA using T4 RNA ligase 2" section (Fig. 2A). Specifically, the linear RNA template was annealed to the guide DNA primer. Then the 5' and 3' of the linear RNA template were connected by T4 RNA ligase 2. Subsequently, the excess DNA ligation primer was eliminated with DNase I. RNase R can digest almost all linear RNA molecules but cannot digest circRNAs. Hence, RNase R digestion was used to demonstrate the feasibility of circRNA synthesis (Fig. 2B). The results showed that the circRNA had higher stability than linear RNA, thus indicating the successful synthesis of circRNA.

Given the special structure of circRNAs, the RT-RCA technique was selected for the amplification of circRNAs. More specifically, some specific reverse transcription primers were designed using the circMUC16 back-splicing site to identify the target. Long ssDNAs with multiple sets of complementary repeats were obtained by RT-RCA and used as the targets of subsequent CRISPR-Cas12a detection (Fig. 2A). The amplification of circRNAs was verified by agarose gel electrophoresis using RT-RCA (Fig. 2C). the molecular weight of cDNAs obtained from purified circRNA was retained. It was found that the concentration of amplified products increased with the extension of reaction time. These results showed that RT-RCA had perfect amplification effects, and the amplification process was completed in approximately 1 h. Moreover, the existence of RT-RCA amplification products was verified. The sequencing results shown in Fig. 2D further demonstrated the selectivity of RT-RCA, as the sequence data were consistent with the circMUC16 sequence. These results confirmed that repeated sequences of cDNAs produced by RT-RCA.

Validation of DCMC-CRISPR

As revealed in a previous study, the assistance of the PAM sequence is not required for Cas12a in detecting ssDNAs. However, in this DCMC-CRISPR experiment,

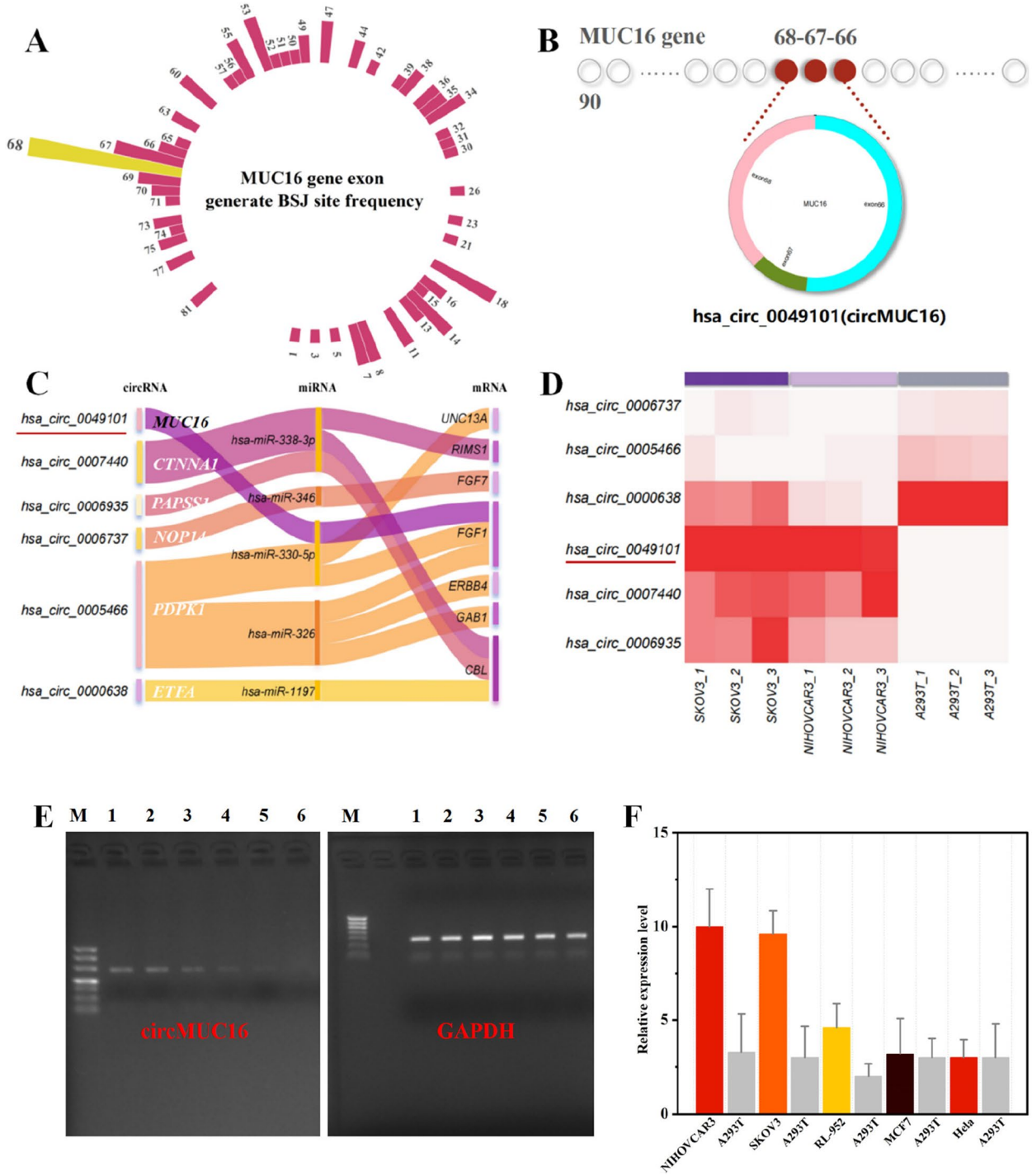

Fig. 1 circMUC16 biomarker screening and validation. **A** The frequency of cirRNA generated from the 90 exons of the MUC16 gene; (**B**) Schematic diagram of the hsa_circ_0049101 (circMUC16); (**C**) Sankey plot of the potential circRNA-miRNA-mRNA; (**D**) Heatmap The expression of circMUC16 in SKOV3 and NIHOVCAR3 cell line; (**E**) The expression of circMUC16 and GAPDH in gynecological cancer cell line (lane 1–5: NIHOVCAR:3, SKOV3, RL952, MCF-7, Hela) and lane 6: normal cell A293T. The products of RT-PCR were analyzed by 1.0% agarose electrophoresis; (**F**) RT-qPCR for circMUC16 expression was used to verify in gynecological cancer cell lines

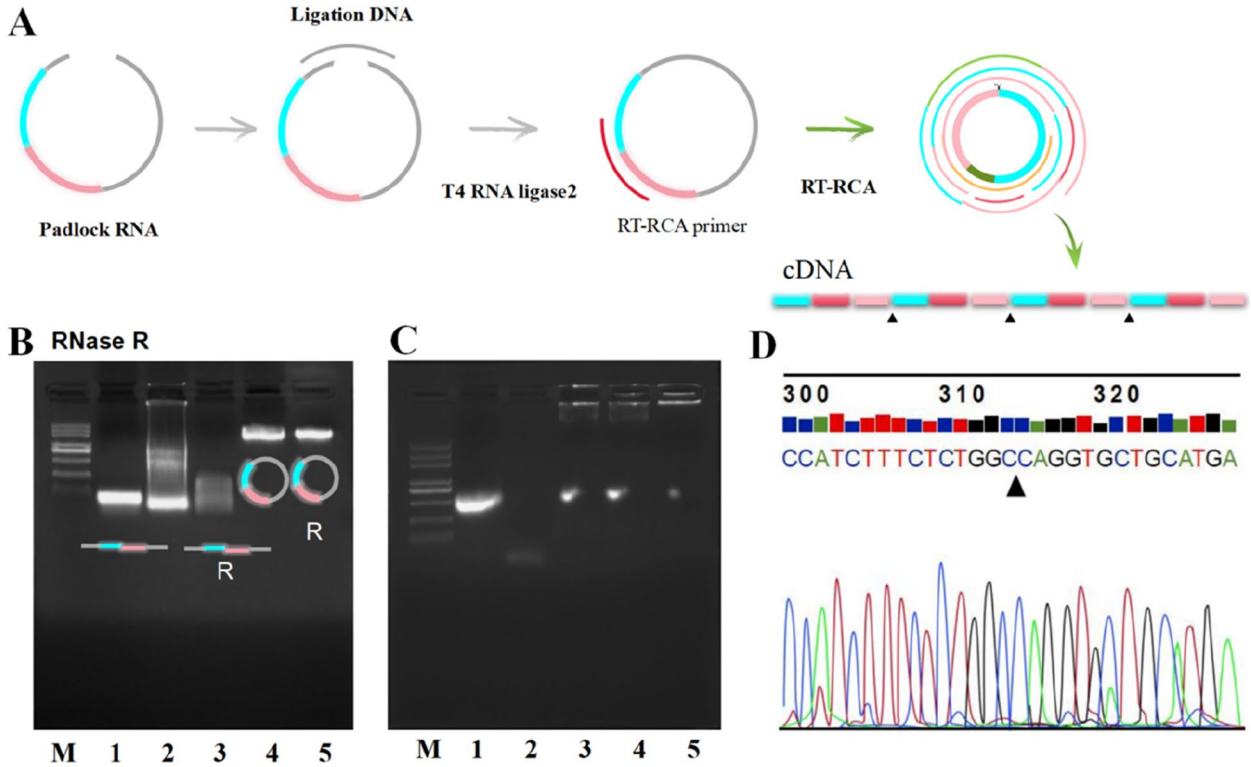

Fig. 2 Validation of the amplification system. **A** Schematic diagram of the circRNA synthesis and RT-RCA preamplification process; (**B**) 1% agarose electrophoresis image for the stability of the circRNA by RNase digestion. Lane M: DL5000 DNA marker, lane 1: linear RNA; lane 2: linear RNA obtained after in vitro transcription, lane 3: RNase R digests linear RNA, lane 4: circRNA, lane 5: RNase R digests circRNA; (**C**)1% agarose electrophoresis image for the RT-RCA process. Lane M:DL5000 DNA marker, lane 1:circRNA, lane 2: RT-RCA primer, lane 3–5: RT-RCA reaction for 1 h, 1.5 h and 2 h; (**D**) Partial sequencing results of PCR products. The emphasis in the figure is the backsplice junction of circMUC16

it was found that the efficiency of the crRNA recognition reaction based on PAM sites was higher than that without the assistance of PAM sequences. As a result, the design of crRNA targeting the PAM site continued (Fig. S2). In this preliminary experiment, given the low sensitivity limit of conventional single protein (Fig. 4A), the homologous protein Francisella strain (FnCas12a) of Lachnospiraceae strain (LbCas12a) was investigated [31, 32]. LbCas12a prefers the PAM sequence recognizing 5'-TTTV-3', and the PAM sequence recognized by FnCas12a can be extended to 5'-TTV-3' [33]. The introduction of FnCas12a can greatly increase the targeting range of Cas12a and the sensitivity of the CRISPR detection. Hence, LbCas12a and FnCas12a were selected in this study to verify the CRISPR/Cas12a system.

The feasibility of the CRISPR/Cas12a system was verified by the following procedures. The specific sequence of FnCas12a crRNA (PAM: TTV) and LbCas12a crRNA (PAM: TTTV) (guide design resource Zhang Lab (zlab.bio)) were designed (Fig. 3A). All crRNAs were synthesized by in vitro transcription at 44 nt and 45 nt, respectively (Fig. 3B). LbCas12a and FnCas12a combined with their detection circRNAs corresponding to crRNAs (LbCas12a/LbcrR1-3 and FnCas12a/FncrR1-3) to compare the sensitivity of six crRNAs (Fig. 3C). When the concentration of circRNAs was 50 pM, these crRNAs can be ranked as LbcrRNA1 > FncrRNA1 > LbcrRNA3 > FncrRNA3 > LbcrRNA2 > FncrRNA2 in order of their detection sensitivity. Then, the crRNA with better performance was selected for combination. As shown in Fig. 3D, LbcrR1, LbcrR3, FncrR1, and FncrR3 have the highest sensitivity.

The feasibility of DCMC-CRISPR was verified by measuring the trans-cleavage activity of LbCas12a/LbcrR1 and FnCas12a/FncrR1 based on the fluorescence dynamics and end-point fluorescence values. The results are shown in Fig. 3E and F, when the RT-RCA product (cDNA) was detected, the fluorescence intensity of LbCas12a/LbcrR1 was higher than that of FnCas12a/FncrR1. This indicated that LbCas12a/LbcrR1 combined with the FnCas12a/FncrR1 detection system significantly improved the detection sensitivity, suggesting that binding Cas12a proteins targeting different PAMs had great potential to enhance the detection sensitivity of circRNAs.

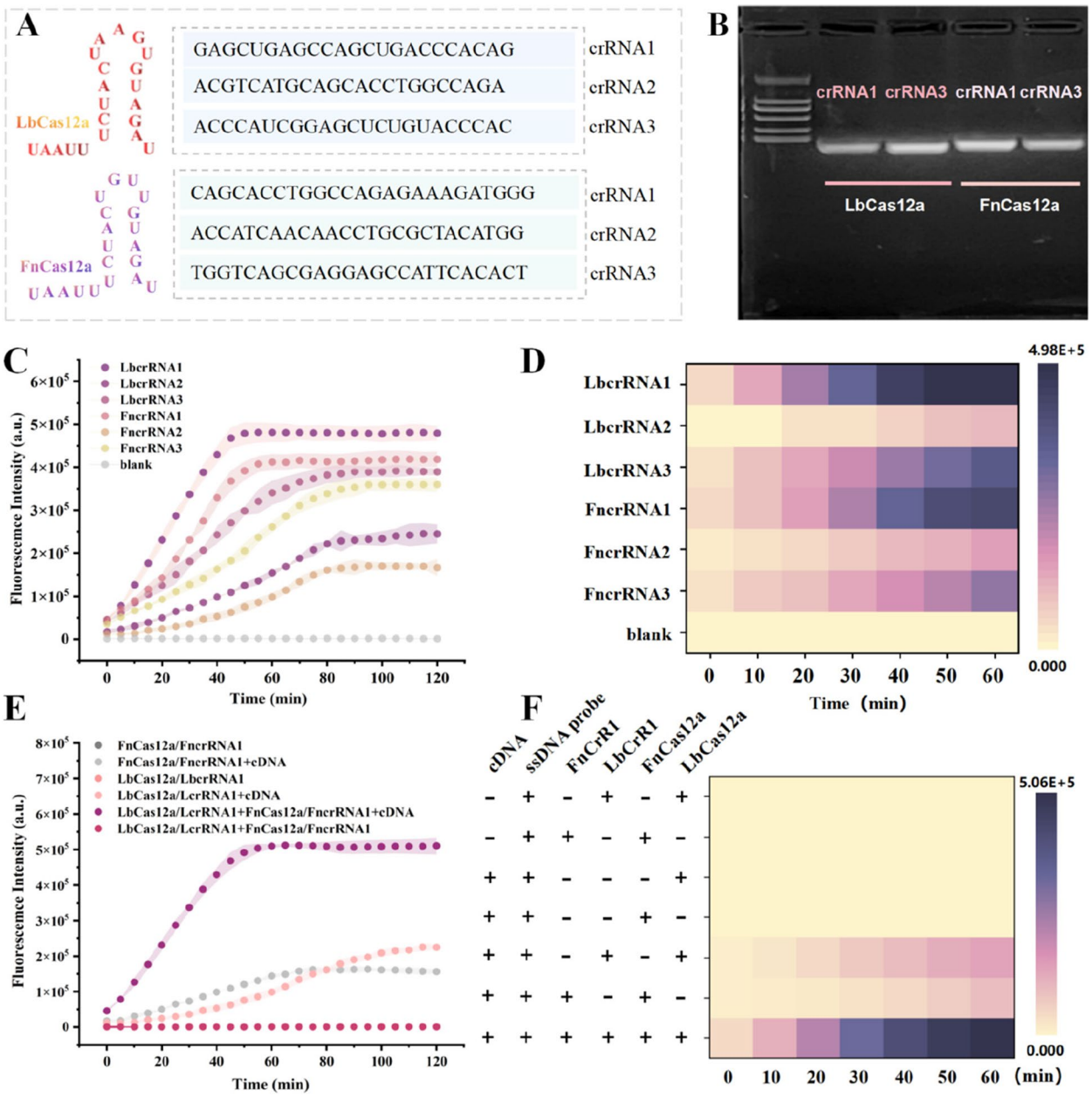

Fig. 3 Validation of the CRISPR/Cas12a system. **A** The secondary structure sequences of the six crRNAs of the LbCas12a and FnCas12a protein; (**B**) crRNAs obtained after in vitro transcription purification, lane M: DL2000 DNA marker; lane 1: LbcrRNA1, lane 2:LbcrRNA3, lane 3: FncrRNA1, lane 4: FncrRNA3; (**C**) Fluorescence kinetics compared the sensitivity of six individual crRNAs to detect circRNA, and the concentration of circMUC16 was set to 50 pM; (**D**) Heatmap of end-point fluorescence values of circRNA from six individual crRNAs; (**E**) Verify the feasibility of CRISPR system to detect circRNA, fluorescence kinetics of FnCas12a/FncrRNA1, LbCas12a/LbcrRNA1 and FnCas12a/FncrRNA1 + LbCas12a/LbcrRNA1 in the presence and absence of target cDNA; (**F**) The heatmap shows the end point fluorescence value to validate the feasibility analysis of CRISPR detection system

Optimization of DCMC-CRISPR

To simplify the testing procedure, a "one-pot" approach was adopted to develop CRISPR-based nucleic acid detection in the initial experiment. However, the RT-RCA reaction significantly interfered with the CRISPR reaction. The results showed that the sensitivity and LOD of the one-step reaction were significantly lower than those of the two-step method (Fig. S3). Therefore, the two-step method was selected to minimize RT-RCA reaction interference effects on the CRISPR reaction.

Then, the RT-RCA amplification step was also optimized (Fig. S4A–C). The results showed that RT-RCA achieved an ideal amplification levels after 40 min, with the primer concentration reaching 480 nM. For CRISPR/Cas12a (Figure S4D–F), CRISPR-based detection is an enzymatic reaction, and the detection capacity is closely related to such parameters as reaction temperature and concentration of enzymes. The ratio of Cas12a to crRNAs and the concentration of Cas12a are important determinants of the reaction speed. The Cas12a-to-crRNA ratio of 1:1 and the concentration of 400 nM yielded the highest fluorescence signal. Cas12a protein can work at 20℃-48℃ and the CRISPR reaction is usually incubated at 37℃ in the pre-amplification combined with the CRISPR-Cas12a detection method. In this study, the CRISPR-Cas12a reaction was incubated at 37℃, 42℃, and 47℃, respectively. It was found that 42℃ was the optimal temperature with a stronger fluorescence response. the optimal operating temperature was 42°C. In summary, the optimal reaction can be achieved under the Cas12a-to-crRNA ratio of 1:1 and the Cas12a concentration of 400 nM at 42°C.

Sensitivity and specificity of DCMC-CRISPR

Based on the above feasibility analysis of CRISPR, the combination of LbCas12a, FnCas12a and their corresponding crRNAs could improve the sensitivity of DCMC-CRISPR in circRNA detection. Therefore, the sensitivity of the combination of different amounts of crRNAs was evaluated in detail to determine the optimal combination of crRNAs.

The Ksv fluorescence quenching efficiency was used to assess the sensitivity of the DCMC-CRISPR assay to circRNA responses. The fluorescence quenching method follows the Stern–Volmer equation:

$$F/F_0 = 1 + K_{SV}C_q \quad (1)$$

where F_0 and F are the fluorescence intensity in the absence and presence of circRNAs, respectively; K_{SV} is the quenching constant of circRNAs.

The target circRNA was serially diluted with a concentration range of 2000–5×10^{-4} pM. Besides, the sensitivity of the DCMC-CRISPR method combined with separate crRNAs, including LbcrRNA1 and LbcrRNA3 (L1 and L3), as well as FncrRNA1 and FncrRNA3 (F1 and F3) were compared (Fig. 4A, Fig. S5). Among them, L1 and F1 showed the highest sensitivity.

Next, two crRNAs were combined in the same reaction (L1 + L3, F1 + F3, L1 + F1, L1 + F3, L3 + F1, and L3 + F3) (Fig. 4B, Fig. S5). The total concentration of the Cas12a/crRNA complex remained constant and was divided equally between each crRNA to maintain the optimal ratio of Cas12a to crRNA (1:1). The binding of crRNAs significantly increased the slope of the detection reaction and the sensitivity of the reaction. It was proved that L1 + F1 exhibited the highest sensitivity, followed by L1 + F3, L3 + F1, and L3 + F3 (Fig. 4E). Besides, the sensitivity of a single Cas12a protein (L1 + L3, F1 + F3) was lower than that of two Cas12a proteins (L1 + F1). The average slope increased almost 3- to fivefold compared with the single crRNA reaction, indicating the advantage of the crRNA combination. Subsequently, the detection sensitivity of the combination including three crRNAs was explored, and the sensitivity of this combinattion was about twofold higher than that of the combination including two crRNAs (Table 1). Based on the above validation results, when four crRNAs (L1 + L3 + F1 + F3) were combined, the detection sensitivity was further improved, more than 4–11 times that of the single and three crRNAs (Fig. 4C, D, Table 1). The heatmap visually compared the endpoint fluorescence values at different concentrations, and the endpoint fluorescence values and slope of each different crRNA combination were analyzed, with the combination including four crRNAs exhibiting the highest sensitivity (Fig. 4F, G).

Under optimal experimental conditions, the sensitivity of DCMC-CRISPR was tested by detecting circMUC16 at various concentrations. The F/F_0 of the fluorescence intensity curve was proportional to the circMUC16 concentration range from 2000 pM to 0.5 fM. The LOD was calculated to be 0.5 fM. The correlation equation

(See figure on next page.)

Fig. 4 Sensitivity of the DCMC-CRISPR system. **A** The single crRNA (L1, F1); (**B**) The two crRNA combinations (L1 + F1, L3 + F1); (**C**) The three crRNA combinations (L1 + L3 + F1, L1 + L3 + F3); (**D**) The four crRNA combinations (L1 + L3 + F1 + F3). Each combination of crRNAs was tested against serial dilutions of circMUC16 (2000, 500, 50, 5, 0.5, 0.05, 0.005 and 0.0005 pM). The end-point fluorescence results are presented. Background fluorescence signals generated by individual Cas12a/crRNA complexes in the absence of target circMUC16 are presented as "NTC"; (**E**) The corresponding linear fitting of FL intensity with logarithmic circMUC16 concentrations (50, 5, 0.5, 0.05, 0.005 and 0.0005 pM) for each combination of crRNAs (1 crRNA, 2crRNA, 3crRNA, 4crRNA). The LOD was calculated by performing linear regression to the fluorescence data integrated from three replicates; (**F**) Results of the endpoint flourscence intensity for each combination of crRNAs detection circMUC16; (**G**) Results of the slope (F/F_0,) for each combination of crRNAs detection circMUC16. The slope of the fluorescence curve was calculated by performing linear regression to data integrated from replicates

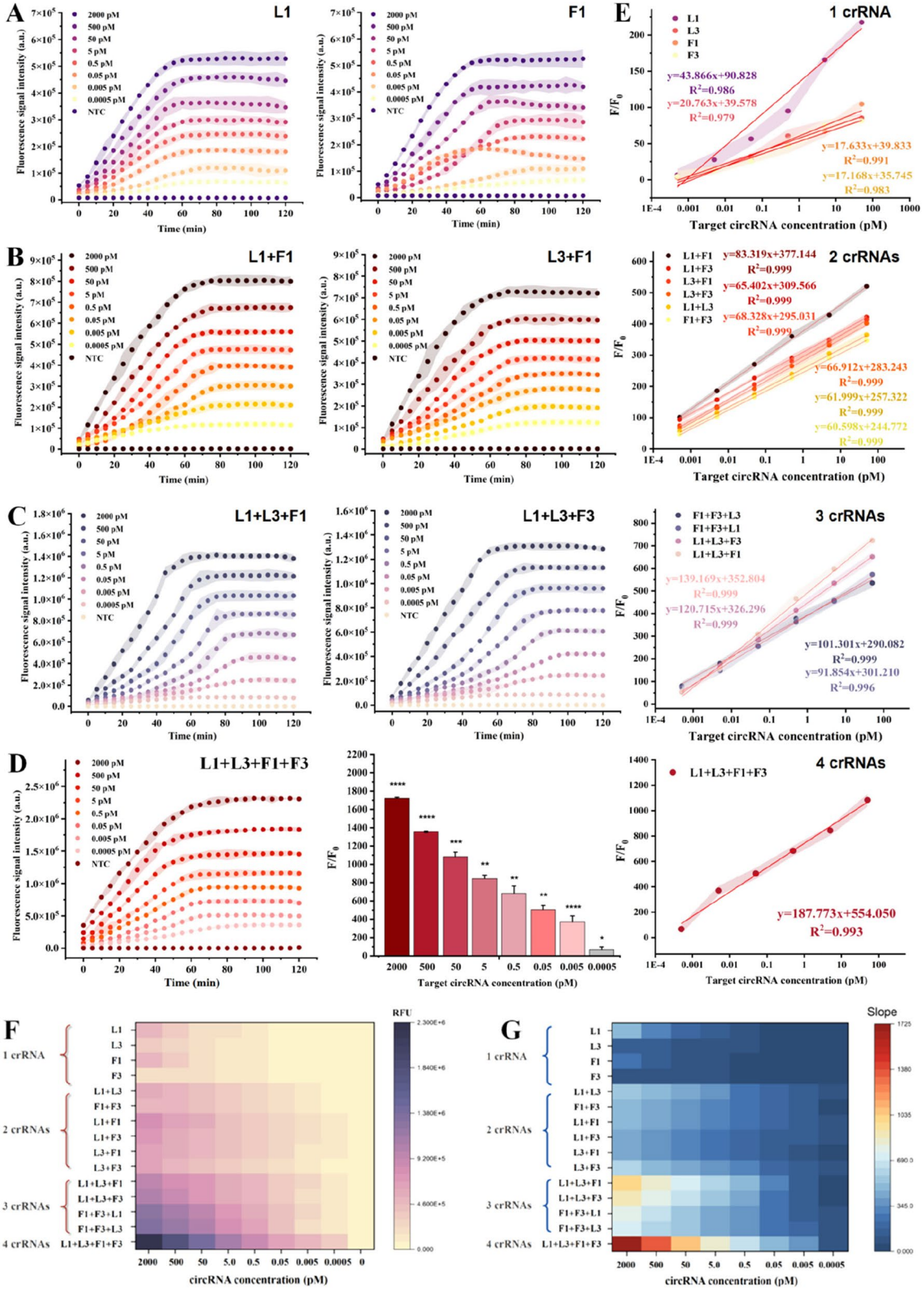

Fig. 4 (See legend on previous page.)

Table 1 Fluorescence quenching constants (*Ksv*) of the DCMC-CRISPR assay under different crRNA combinantions

Combinations	*ksv*	Combinations	*ksv*	Combinations	*ksv*
L1	43.866	L1 + F3	65.402	F1 + F3 + L3	101.301
F1	20.763	L3 + F1	68.328	F1 + F3 + L1	91.854
L3	17.633	L3 + F3	66.912	L1 + L3 + F3	120.712
F3	17.168	L1 + L3	61.999	L1 + L3 + F1	139.169
L1 + F1	83.319	F1 + F3	60.598	L1 + L3 + F1 + F3	187.773

was obtained as $y = 787.948 + 242.077\log C$ ($R^2 = 0.964$) (Fig. 4E, Fig. S6A). Compared with the recently reported results of fluorescence methods for circRNA detection listed in Table S3, the LOD of this method was at least 100-fold lower than that using a single Cas12a protein or other electrochemical and fluorescence methods. Further, its sensitivity was comparable to that of the DSN/TdT-Assisted Cascade Signal Amplification method. This suggested that this method was significantly superior to other detection methods.

The combination of multiplex crRNAs improved the detection sensitivity. However, when the number of crRNA increased to 5 and 6, the signal response and curve slope could not increase continuously (Fig. S6B). In summary, these results demostrated that the DCMC-CRISPR combining two Cas12a proteins targeting different PAM sites and their corresponding four crRNAs (L1, L3, F1, and F3) enhanced the highest sensitivity of the circMUC16 detection system.

The specificity and anti-interference performance of this detection method was also evaluated in this study. The ability of this assay to distinguish between single-base mismatches was verified using the LbcrRNA3 sequence. The fluorescence intensity of the perfectly matched LbcrRNA3 was approximately twice as much as M-1 and about six times as much as M-5 (Fig. 5A, B). Next, circRNAs were mixed with linear RNA in ratios of 1:5, 1:50 and 1:500 to evaluate the anti-interference ability (Fig. 5C, D). Mixing with a high concentration of linear RNA did not affect the detection efficiency of circRNA. There were no statistical differences between circRNA and the mixtures with linear RNA. Additionally, the cell specificity was also verified. It was found that circMUC16 in NIH:OVCAR3 cells showed a strong fluorescence intensity, with some expression in SKOV3 (Fig. 5E, F). These results indicated that this method had excellent cell specificity, and this detection method can distinguish single base mutation and had high specificity and favorable anti-interference abilities.

Detection mechanisms of DCMC-CRISPR

To clarify the detection mechanism of DCMC-CRISPR, the detection efficiency of LbCas12a and FnCas12a were compared at the TTTV and TTV PAM sites, respectively. In Fig. 6A, the highly conserved circRNA BSJ sequence was selected as the amplification region, and the amplified product cDNA was used as the Cas12a/crRNA binding region. The crRNA was designed in different sites in the same amplification region. A total of six crRNAs restricted by the TTTV PAM site (TTTV site1, TTTV site2, and TTTV site3) and the TTV PAM site (TTV site1, TTV site2, and TTV site3) were designed in this study. LbCas12a and FnCas12a were individually combined with these six crRNAs to detect RT-RCA product cDNA target.

At the TTV PAM site, FnCas12a exhibited the highest detection efficiency, followed by LbCas12a protein. The relatively low detection efficiency of LbCas12a may be attributed to its strict recognition of the "TTTV" 4-base PAM site. The failure to accurately locate the target at the TTV PAM site caused a reduction in the detection efficiency (Fig. 6B, D). At the TTTV PAM site, the endpoint fluorescence value showed that Lbcas12a and FnCas12a were both highly active at the "TTTV" 4-base PAM site (Fig. 6C, E), and the detection efficiency of LbCas12a was relatively higher compared with FnCas12a. However, the fluorescence intensity of LbCas12a at the TTV PAM site was relatively lower than that in TTTV PAM, which limited the effective range of crRNAs. Therefore, based on LbCas12a protein, the introduction of FnCas12a can achieve perfect complementarity with LbCas12a at the targeted PAM site, which significantly expanded the targetable range of Cas12a protein, thus greatly improving the detection sensitivity.

From the above, LbCas12a and FnCas12a can complement each other, and the corresponding crRNA combination displayed detection advantages. For two crRNAs, such as L1 + F1, and four crRNAs L1 + L3 + F1 + F3, the detection sensitivity was significantly improved compared with the single crRNA. However, the sensitivity did not increase with an increase in the number of crRNA (Fig. S6). Limited by the short length of circMUC16 (only 334 bp), there are only six available TTTV and TTV PAM sites. The combination of L2 + F1 and F2 + F3 overlapped with each other in the target sequence, which

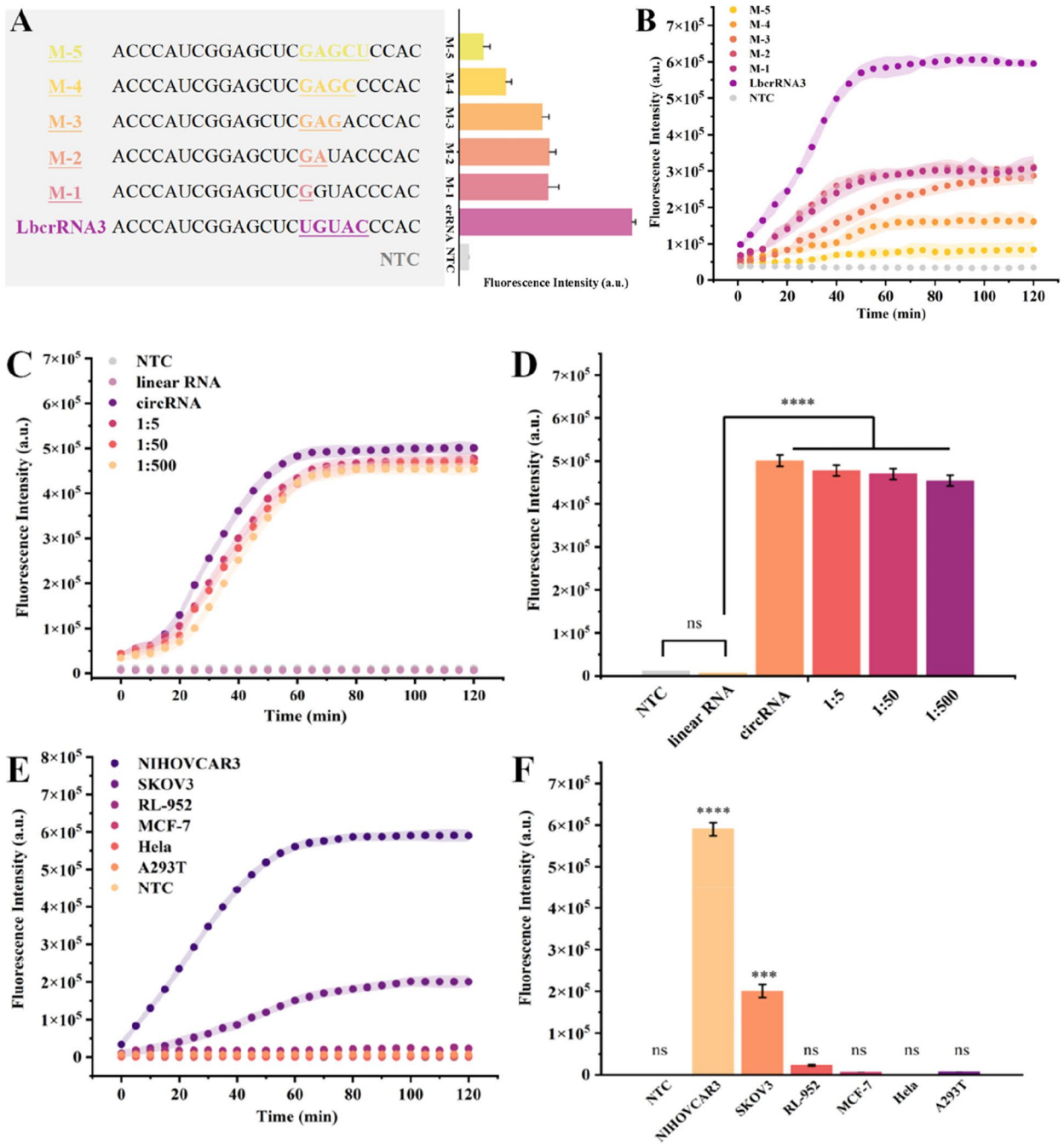

Fig. 5 Specificity and applicability of the DCMC-CRISPR assay. **A** Mismatch sequence and corresponding bar diagram; (**B**) Fluorescence kinetics diagram by one-base mismatched assistant crRNA (M-1), two-base mismatched crRNA (M-2), three-base mismatched crRNA (M-3), Four-base mismatched crRNA (M-4), Five-base mismatched crRNA (M-5), LbcrRNA 3 (NTC); (**C**) Fluorescence kinetics diagram and (**D**) Fluorescence intensity histogram for different concentrations of circRNA in different cell matrixes; (**E**) Fluorescence kinetics diagram and (**F**) Fluorescence intensity histogram for the evaluation of anti-interference ability by mixture of circRNA and linear RNA. Error bars represent standard deviations for three technical replicates

resulted in insufficient efficiency in the detection containing the above combination (Fig. S7). Therefore, the detection mechanism research results corroborated that the sensitivity of the CRISPR detection system combining various proteins and multiplex crRNAs was closely related to the PAM site and the position of crRNAs.

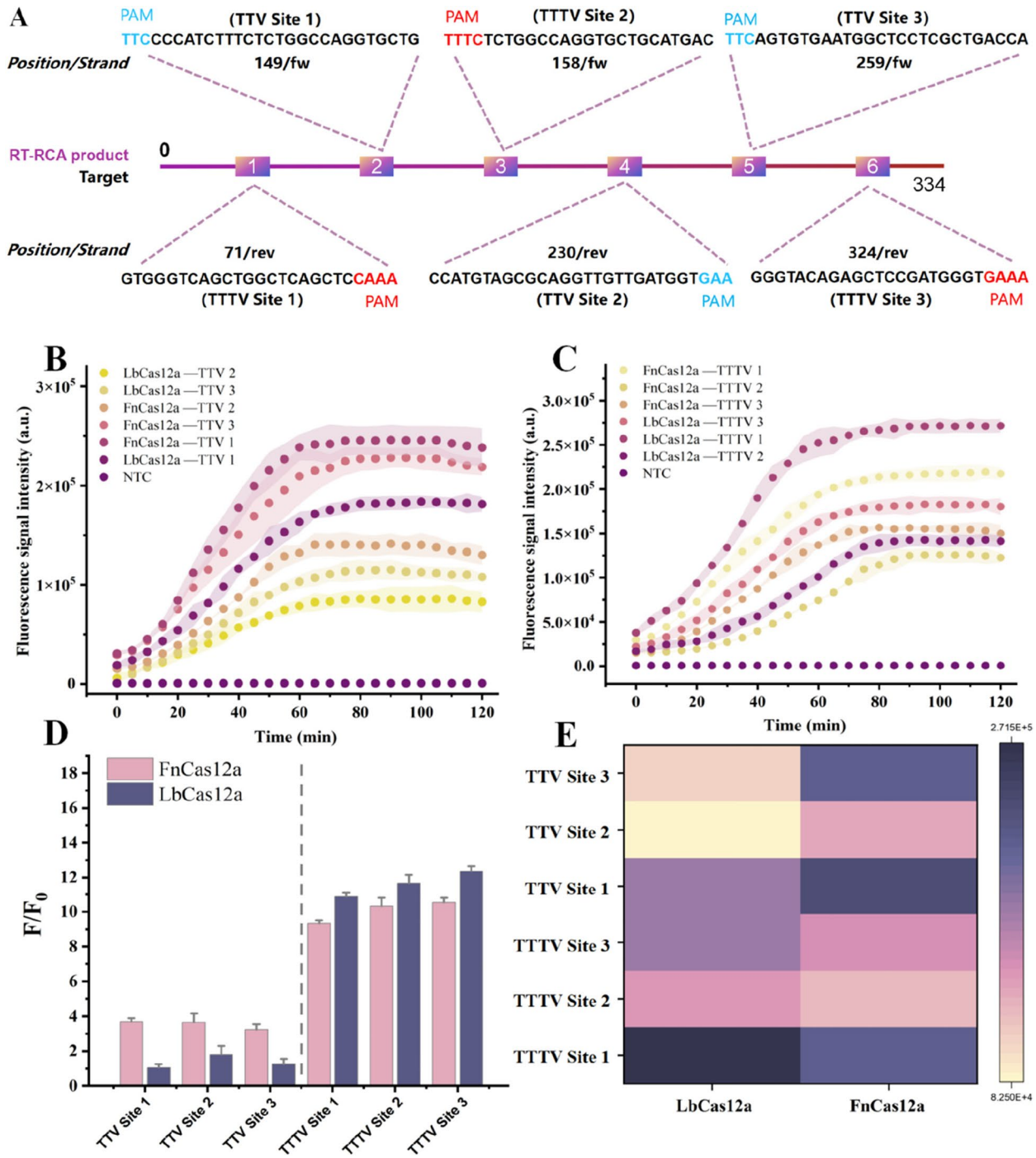

Fig. 6 Investigate the mechanism of the DCMC-CRISPR system. **A** Schematic illustration of LbCas12a and FnCas12a six designed crRNAs (TTV site1-3,TTTV site1-3) targeted regions; (**B**) The fluorescence dynamics of LbCas12a and FnCas12a protein couple with three crRNAs (TTV site1-3) detection circMUC16 (0.5 pM); (**C**) The fluorescence dynamics of LbCas12a and FnCas12a protein couple with three crRNAs (TTTV site1-3) detection circMUC16 (0.5 pM). Background fluorescence signals generated by individual Cas12a/crRNA complexes in the absence of target circMUC16 are presented as "NTC"; (**D**) Bar graph of the detection efficiency (F/F_0) of the two proteins at different PAM sites; (**E**) Heatmap graph of the detection circMUC16 endpoint flourscence intensity of the two proteins at different PAM sites

Testing of clinical samples

To further evaluate the clinical applicability of the circMUC16 biomarker and DCMC-CRISPR assay, the DCMC-CRISPR and RT-qPCR strategy were used to quantify circMUC16 in clinical blood samples from 28 healthy controls and 22 OC patients. Besides, the results of circMUC16 were compared with those of clinical routine serum markers, including CA-125, HE4, and ROMA index. CA-125, HE4, and ROMA index were detected by conventional enzyme-linked immunosorbent assay (ELISA), with the results presented in scatter plots. The coefficient of variation (CV) is a statistical measure exhibiting the dispersion of the test data from the same batch of samples.

The extracted RNA from clinical samples was analyzed by DCMC-CRISPR and RT-qPCR (Fig. 7A). The DCMC-CRISPR method can correctly identify most of the positive cases (Fig. 7B, Fig. S8). The results shown that the concentration of FIGO stage IV malignant tumor samples (#9, #11, #12, #17, #18, #19, #20, #21) and stage III malignant tumor samples (#1, #2, #3, #6, #13, #14, #15, #16 #22) (Fig. S8, Table S2) were higher than that early stage tumor samples (stage II #4, #5, #7, #8, and stage I #10). The RT-qPCR results showed that the threshold

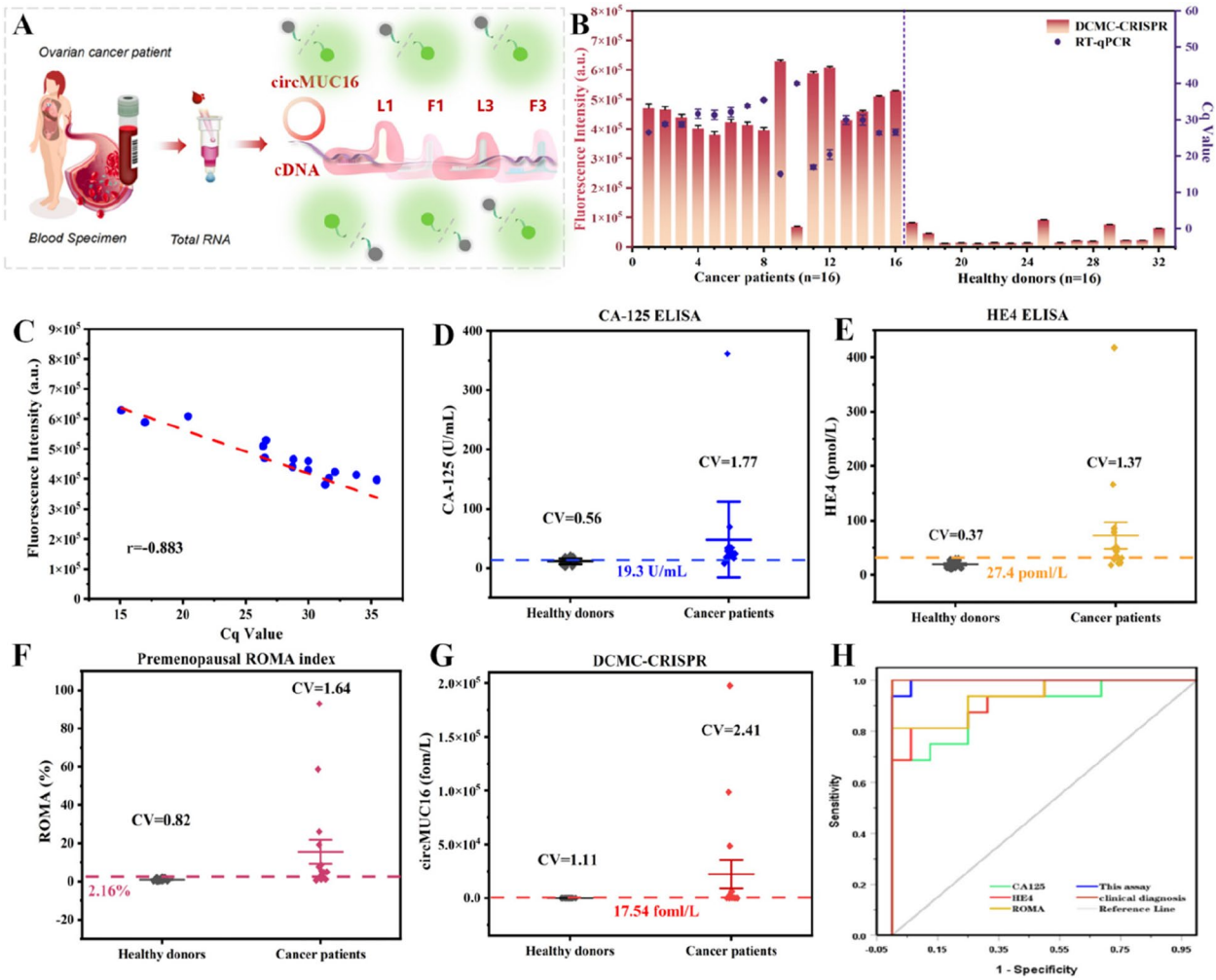

Fig. 7 Analysis of clinical samples (**A**) Schematic of clinical diagnosis of circRNA using the DCMC-CRISPR; (**B**) RT-qPCR and DCMC-CRISPR examined blood samples from 22 clinical ovarian cancer patients and 28 healthy donors; (**C**) Correlation analysis between RT-qPCR and the developed DCMC-CRISPR; (**D**) Scatter diagrams of CA-125 level determined by ELISA from normal control ($n=28$) and patients of ovarian cancer ($n=22$); (**E**) Scatter diagrams of HE4 level determined by ELISA from normal control ($n=28$) and patients of ovarian cancer ($n=22$); (**F**) Scatter diagrams of ROMA level determined by ELISA from normal control ($n=28$) and patients of ovarian cancer ($n=22$); (**G**) Scatter plots of circMUC16 level by the established assay between cancer patients ($n=22$) and healthy donors ($n=28$); (**H**) ROC curve analysis between normal control and patients of ovarian cancer by the developed assay, CA125 ELISA, HE4 ELISA and ROMA index. AUC: area under the curve. Coeffcient of variation CV = (SD/Mean) × 100%

number of cycles (Ct) for circMUC16 was between 15.086 and 35.438 in all positive samples, while no circMUC16 was detected in most of the negative samples. Trace amounts of circMUC16 were detected in Sample #10, with a low fluorescence intensity and high Ct value of 39.9. A Pearson correlation coefficient of 0.712 indicated that DCMC-CRISPR was highly consistent with RT-qPCR (Fig. 7C).

The level of CA-125 ranged from 8.1 U/mL to 535.10 U/mL in OC samples, and from 1.3 U/mL to 72.6 U/mL in control samples (Fig. 7D). The ELISA results showed that CA-125 was quite dispersed in OC patients (CV = 1.48) and healthy populations (CV = 0.85). When the cutoff value was 20.7 U/mL, there were one false positive (Samples #24) in the healthy samples and five false negatives below the cutoff (Samples #3, #5, #10, #12, and #13) in the OC samples (Table S2). These results indicated that the blood sample from healthy controls had a certain amount of CA-125 that was not distinguishable from OC patients. Thus, CA-125 was not suitable for identifying OC. HE4 exhibited higher sensitivity compared with CA-125. In this study, HE4 ELISA was conducted to distinguish OC samples from normal samples (Fig. 7E, Table S2). It was found that the level of HE4 in the OC samples determined by ELISA ranged from 18.2 pmol/L to 165.9 pmol/L (CV = 1.18), while the concentration of HE4 in the control samples ranged from 0.6 pmol/L to 74.3 pmol/L (CV = 0.68). The sensitivity of the ROMA index were superior to those of CA125 and HE4. The ROMA index ranged from 0.69% to 92.97% (CV = 1.40) for OC patients and 0.17% to 17.13% (CV = 1.30) for healthy controls (Fig. 7F, Table S2).

The patients selected in this study were mainly composed of premenopausal women, and the premenopausal ROMA index can be calculated as follows:

Premenopausal

$$\mathrm{PI} = -12.0 + (2.38 \times \mathrm{LN}(\mathrm{HE4})) + (0.0626 \times \mathrm{LN}(\mathrm{CA125})) \quad (2)$$

Predicted probability

$$\mathrm{ROMA}(\%) = 100 \times \frac{\mathrm{Exp}(\mathrm{PI})}{1 + \mathrm{Exp}(\mathrm{PI})} \quad (3)$$

Based on the DCMC-CRISPR strategy, the level ranged from 6.9×10^{-4} fmol/L to 19.76×10^{4} fmol/L (CV = 2.02) in OC samples,and from 0.82×10^{-4} to 12.59×10^{-4} fmol/L (CV = 1.64) in healthy samples (Table S2). The sensitivity and specificity of this method were 95.5% and 100%, respectively. However, it has a relatively high CV value (Fig. 7G), which may be explained by that the samples were intermixed with terminal malignant and early stage cases. However, the level of circMUC16 from most OC patients was significantly higher than healthy controls. Only the early stage I sample #10 yielded false negative results, which was consistent with the RT-qPCR result. This method represented a potential clinical application for the early screening of OC.

The sensitivity and specificity of DCMC-CRISPR were evaluated using the ROC curve and compared with the ELISA results (Fig. 7H, Table 2). In ELISA, the sensitivity and specificity of CA-125 were 77.3% and 96.4%, respectively (AUC, 0.883). The sensitivity and specificity of HE4 were 81.8%, and 67.9%, respectively (AUC, 0.793). When the cutoff value was 2.16%, the assessment based on the ROMA index had three false negative results. The sensitivity and specificity of the ROMA index were 86.4% and 64.3%, respectively (AUC, 0.789). Notably, the sensitivity and specificity of circMUC16 detected by DCMC-CRISPR were 95.5% and 100%, respectively, (AUC, 0.979). It should be noted that these findings were derived from a limited cohort of 50 clinical samples, and subsequent validation with expanded sample sizes is required to mitigate potential deviations in performance metrics. Furthermore, the ROC curves indicated that DCMC-CRISPR and circMUC16 can effectively detect early-stage OC, with the specificity reaching 100%. The above results further confirmed that circMUC16 was a potent biomarker and DCMC-CRISPR was a promising application protocol for screening OC patients at an early stage with higher specificity and sensitivity.

Table 2 AUCs, Sensitivities, and Specificities of the DCMC-CRISPR assay, CA-125 ELISA, HE4 ELISA techniques and ROMA index for clinical ovarian cancer diagnosis

		AUC (95% CI)	Cutoff value	Sensitivity % (95% CI)	Specificity % (95% CI)
OV versus NC	DCMC-CRISPR (fmol/L)	0.979	> 17.545	95.5	100
	ELISA (CA-125 (U/mL))	0.883	> 20.70	77.3	96.4
	ELISA (HE4 (pmol/L))	0.793	> 29.40	81.8	67.9
	ELISA (ROMA (%))	0.789	> 2.160	86.4	64.3

CI Confidence interval

Discussion

The sensitive and effective screening of patients with ovarian cancer (OC) at an early stage is crucial for the prevention, diagnosis, and treatment of this malignancy. In particular, identifying efficient and feasible nucleic acid biomarkers and constructing relevant detection methods to predict the occurrence of early OC are expected to revolutionize the diagnosis and treatment of this cancer [34]. In this study, high-efficiency biomarkers for OC were screened and DCMC-CRISPR with higher sensitivity and specificity was constructed to detect circRNA biomarkers in OC. Firstly, circRNA biomarkers were screened using data mining and circRNA sequencing (circRNA-Seq). Besides, these circRNA biomarkers were validated in cell and clinical samples using RT-qPCR and the DCMC-CRISPR. Meanwhile, a DCMC-CRISPR strategy for the sensitive and specific detection of circRNA biomarkers in OC was also established in this study. Moreover, a detection method based on RT-RCA combined with CRISPR-Cas12a was constructed using the two-step detection method, which avoided the sensitivity reduction caused by multi-enzyme interference in the one-pot method and averted poor compatibility. Based on the biosensing technology of CRISPR, Cas nucleases can identify the target genes by cleaving the crRNA complementary to the target and the short sequence protospacer adjacent motif (PAM) flanking the target [35, 36]. A single Cas protein and a single crRNA are commonly used in conventional CRISPR detection methods, which makes crRNA strictly limited by PAM sites in design. In addition, the flexibility of PAM sequences significantly limits the range of Cas nucleases that can be targeted, thus reducing the detection sensitivity [37, 38]. Based on LbCas12a, the introduction of FnCas12a targeting TTV sites can achieve perfect complementarity with LbCas12a at the targeted PAM site, which significantly expanded the targetable range of Cas12a proteins, thus greatly improving the detection sensitivity [39]. At the same time, four crRNAs corresponding to the two Cas12a proteins were designed, and the four crRNAs that were verified and screened were evenly distributed on the target sequence, avoiding competitive detection in the spatial position. Therefore, the binding of multiple crRNAs for the two proteins further increased the detection efficiency of circRNAs, and the minimum circRNAs at the fM level can be detected, thus realizing the ultra-sensitive detection of circRNAs. The detection mechanism of CRISPR-Cas12a technology was also verified by multiple designs of crRNAs at different PAM sites. The results confirmed the influence of PAM sites on Cas12a sensitivity.

The successful detection of circRNA biomarkers by DCMC-CRISPR in clinical samples demonstrated its potential to optimize other nucleic acid molecular diagnostic applications. In particular, the programmability of DCMC-CRISPR can be used to detect biomarkers in different disease courses, especially in the context of precision medicine and personalized diagnosis and treatment. In the future, the DCMC platform can also be further applied to the combined detection of multiple biomarkers to assist in more targeted therapies.

However, there are some limitations for the DCMC-CRISPR platform. Firstly, the reduced sensitivity during the one-pot detection of the circRNA amplification phase and CRISPR detection phase was detected in evaluating the feasibility of this method.. This can be attributed to the multiple enzyme systems in different systems with mutual interference between amplification and detection processes. This limitation highlights the necessity for further balancing the circRNA amplification step and the CRISPR detection step, thus reducing the detection time. Secondly, the DCMC-CRISPR strategy involves complex extraction steps of blood RNA extraction step, and several sequential steps. which, while manageable, can still be a bottleneck in resource-limited settings. Simplifying and streamlining sample preparation procedures can improve the applicability of this method for point-of-care applications.

Regarding clinical validation, while achieving perfect specificity (100%) in distinguishing ovarian cancer patients from matched controls ($n=50$) is noteworthy, the limited cohort size restricts statistical power for assessing population-level biological variability. Future validation should prioritize large-scale multi-center studies to ensure robust generalizability of the diagnostic parameters.

To simplify this process, a method is envisioned to further integrate sample RNA extraction and purification and DCMC-CRISPR methods onto microfluidic chips, and magnetic beads may be designed to purify and enrich circRNAs in samples at the time of sample addition. Further, the required CRISPR and RT-RCA components can be loaded into their respective chambers in the freeze-dried form. This innovation may greatly simplify the workflow, which may enhance the feasibility of the platform in real point-of-care testing (POCT) applications.

Conclusions

In summary, an effective biomarker circMUC16 (hsa_circ_0049101) was identified in this study, and an ultra-sensitive DCMC-CRISPR strategy was also constructed for the detection of circMUC16. This strategy utilized RT-RCA pre-amplification target circRNAs and dual Cas12a proteins (LbCas12a and FnCas12a) targeting different PAM sites, and the corresponding multiplex crRNAs were also employed to overcome the limited sensitivity of LbCas12a by TTTV PAM sites. DCMC-CRISPR has 4–11 times higher sensitivity than the

single-crRNA CRISPR/Cas12a system. The developed strategy exhibited a broad detection range from 2000 pM to 0.5 fM, and a low detection limit of 0.5 fmol/L, which was 10^2–10^4 times lower than that of most detection methods reported recently. Furthermore, the developed DCMC-CRISPR assay exhibits the capacity to distinguish ovarian cancer patients from healthy controls with high specificity in the current sample collection, while its clinical translation would necessitate further validation through expanded cohort studies. This method outperformed CA-125 and HE4 and was comparable with RT-qPCR and the ROMA index. Furthermore, these results validated that circMUC16 can serve as a potential early diagnostic biomarker for OC. This circRNA biomarker and the DCMC-CRISPR strategy are expected to furnish the potential application in the monitoring of cancer progression in clinical practice.

Abbreviations

OC	Ovarian cancer
CA125	Carcinoma Antigen 125
HE4	Human Epididymis Protein 4
ROMA index	Risk of Ovarian Malignancy Algorithm index
RT-RCA	Reverse Transcription Rolling Circle Amplification
CRISPR	Clustered Regularly Interspaced Short Palindromic Repeats
Cas	CRISPR-associated
DCMC-CRISPR	Dual Cas12a Multiple CrRNA-CRISPR
L1	LbCas12a crRNA1
L3	LbCas12a crRNA3
F1	FnCas12a crRNA1
F3	FnCas12a crRNA3

Supplementary Information

The online version contains supplementary material available at https://doi.org/10.1186/s12885-025-14116-w.

Supplementary Material 1.

Supplementary Material 2.

Acknowledgements
We thank Dr. Gabrielle White Wolf, from Liwen Bianji (Edanz) (www.liwenbianji.cn) for editing the English text of a draft of this manuscript.

Authors' contributions
Lingxi Tian: Data curation, Writing—original draft preparation. Jun Yang: Supervision, Writing—review & editing. Lihan Zi: Methodology. Yan Gao: Supervision. Lingxi Tian: Validation; Ruilian Zhe: Visualization.

Funding
This work was supported by the Dalian Science and Technology Innovation Fund (2022JJ12SN049), the Fundamental Research Funds for the Central Universities (DUT22YG121, DUT22YG243).

Data availability
No datasets were generated or analysed during the current study.

Declarations

Ethics approval and consent to participate
The experimental protocol was established, according to the ethical guidelines of the Helsinki Declaration and was approved by the Human Ethics Committee of Liaoning Cancer Hospital & Institute (Shenyang, Liaoning, China) and Dalian university of technology (Dalian, Liaoning, China). Written informed consent was obtained from individual or guardian participants.

Consent for publication
Not applicable.

Competing interests
The authors declare no competing interests.

Received: 22 June 2024 Accepted: 8 April 2025
Published online: 15 April 2025

References

1. Jayson GC, Kohn EC, Kitchener HC, Ledermann JA. Ovarian cancer. Lancet. 2014;384(9951):1376–88.
2. McMullen M, Karakasis K, Rottapel R, Oza AM. Advances in ovarian cancer, from biology to treatment Nat. Cancer. 2021;2(1):6–8.
3. Llauradó M, Majem B, Altadill T, Lanau L, Castellví J, Sánchez-Iglesias JL, et al. MicroRNAs as prognostic markers in ovarian cancer. Mol Cell Endocrinol. 2022;390(1–2):73–84.
4. Palmqvist C, Staf C, Mateoiu C, Johansson M, Albertsson P, Dahm-Kähler P. Increased disease-free and relative survival in advanced ovarian cancer after centralized primary treatment. Gynecol Oncol. 2020;159(2):409–17.
5. Tian W, Zhou Y, Wu M, Yao Y, Deng Y. Ovarian metastasis from breast cancer: a comprehensive review. Clin Transl Oncol. 2019;21(7):819–27.
6. Hen SLP, Yang AQ, Jin L. Strumal carcinoid tumor of the ovary: report of rare occurrence with review of literature. Diagnostics. 2022;12(11):2706–19.
7. Dochez V, Caillon H, Vaucel E, Dimet J, Winer N, Ducarme G. Biomarkers and algorithms for diagnosis of ovarian cancer: CA125, HE4, RMI and ROMA, a review. J Ovarian Res. 2019;12(28):2–9.
8. Qing XL, Liu LT, Mao XG. A Clinical Diagnostic Value Analysis of Serum CA125, CA199, and HE4 in Women with Early Ovarian Cancer: Systematic Review and Meta-Analysis. Comput Math Methods Med. 2022;9339352:10.
9. Lycke M, Kristjansdottir B, Sundfeldt K. A multicenter clinical trial validating the performance of HE4, CA125, risk of ovarian malignancy algorithm and risk of malignancy index. J Gynecol Oncol. 2018;151(1):159–65.
10. Irajizad E, Han CY, Celestino J, Wu RR, Murage E, Spencer R, et al. A Blood-Based Metabolite Panel for Distinguishing Ovarian Cancer from Benign Pelvic Masses. Clin Cancer Res. 2022;28(21):4669–76.
11. Davenport CF, Rai N, Sharma P, Deeks J, Berhane S, Mallett S, et al. Diagnostic Models Combining Clinical Information. Ultrasound and Biochemical Markers for Ovarian Cancer: Cochrane Systematic Review and Meta-Analysis, Cancers. 2022;14(15):3621–36.
12. Moore RG, McMeekin DS, Brown AK, DiSilvestro P, Miller MC, Allard WJ, et al. A novel multiple marker bioassay utilizing HE4 and CA125 for the prediction of ovarian cancer in patients with a pelvic mass. Gynecol Oncol. 2009;112(1):40–6.
13. Molina R, Escudero JM, Augé JM, Filella X, Foj L, Torné A, et al. HE4 a novel tumour marker for ovarian cancer: comparison with CA125 and ROMA algorithm in patients with gynaecological diseases. Tumour Biol. 2011;32(6):1087–95.
14. Ghafouri-Fard S, Hussen BM, Taheri M, Ayatollahi SA. Emerging role of circular RNAs in breast cancer. Pathol Res Pract. 2021;223:153496.
15. Liu CX, Chen LL. Circular RNAs: Characterization, cellular roles, and applications. Cell. 2022;185(13):2016–34.
16. Zhang WJ, Chen X, Yang ZP, Zhou JS, Peng W, et al. Circular RNAs in tumor immunity and immunotherapy. Mol Cancer. 2024;23(171):4365–7.
17. Hansen TB, Jensen TI, Clausen BH, Bramsen JB, Finsen B, Damgaard CK, et al. Natural RNA circles function as efficient microRNA sponges. Nature. 2013;495(7441):384–8.
18. Meng SJ, Zhou HC, Feng ZY, Xu ZH, Tang Y, Li PY, et al. CircRNA: functions and properties of a novel potential biomarker for cancer. Mol Cancer. 2017;16(1):94.
19. Wu MT, Qiu QZ, Zhou Q, Li J, Yang JZ, Zheng CC, et al. circFBXO7/miR-96–5p/MTSS1 axis is an important regulator in the Wnt signaling pathway in ovarian cancer. Mol Cancer. 2022;21(1):137.

20. Gan X, Zhu H, Jiang X, Obiegbusi SC, Yong M, Long X, et al. CircMUC16 promotes autophagy of epithelial ovarian cancer via interaction with ATG13 and miR-199a. Mol Cancer. 2020;19(1):1–13.
21. Marieke V, Nurten Y, Kimberly V, Steve L, Jo V, Jan VP. Validation of circular RNAs using RT-qPCR after effective removal of linear RNAs by Ribonuclease R. Curr proto. 2021;1(7):181.
22. Zhang XL, Zhao YJ, Zeng Y, Zhang CY. Evolution of the probe-based loop-mediated isothermal amplification (LAMP) assays in pathogen detection. Diagnostic. 2023;13(9):1530–55.
23. Bialy RM, Mainguy A, Li YF, Brennan JD. Functional nucleic acid biosensors utilizing rolling circle amplification. Chem Soc Rev. 2022;51(21):9009–67.
24. Zetsche B, Gootenberg JS, Abudayyeh OO, Slaymaker IM, Makarova KS, Essletzbichler P, et al. Cpf1 is a single RNA-guided endonuclease of a class 2 CRISPR-Cas system. Cell. 2015;163(3):759–71.
25. Bravo JPK, Hallmark T, Naegle B, Beisel CL, Jackson RN, Taylor DW. RNA targeting unleashes indiscriminate nuclease activity of CRISPR-Cas12a2. Nature. 2023;613(7944):582–7.
26. Chen JS, Ma EB, Harrington LB, Da Costa M, Tian XR, Palefsky JM, et al. CRISPR-Cas12a target binding unleashes indiscriminate single-stranded DNase activity. Science. 2018;360(6387):436–9.
27. Li HX, Wang Y, Wan Y, Li MM, Xu JG, Wang Q, et al. Stimuli-responsive incremental DNA machine auto-catalyzed CRISPR-Cas12a feedback amplification permits ultrasensitive molecular diagnosis of esophageal cancer-related microRNA. Talanta. 2024;271(1):125675–83.
28. Lu Z, Ni W, Liu N, Jin D, Li TX, Li K, et al. CRISPR/Cas12a-based fluorescence biosensor for detection of exosomal miR-21 derived from lung cancer. Micro Chem. 2023;187:108370.
29. Chen XL, Huang CW, Zhang J, Hu Q, Wang D, You QY, et al. Mini crRNA-mediated CRISPR/Cas12a system (MCM-CRISPR/Cas12a) and its application in RNA detection. Talanta. 2023;268(1):125350–8.
30. Lee DH, Choi S, Park Y, Jin HS. Mucin1 and Mucin16: Therapeutic Targets for Cancer Therapy. Pharmaceuticals. 2021;14(10):1053.
31. Moreno-Mateos MA, Fernandez JP, Rouet R, Vejnar CE, Lane MA, Mis E, et al. CRISPR-Cpf1 mediates efficient homology-directed repair and temperature-controlled genome editing. Nat Commun. 2024;8:2017.
32. Liu XX, Liu XY, Zhou CC, Lv JN, He XB, Liu YY, et al. Engineered FnCas12a with enhanced activity through directional evolution in human cells. Biol Chem. 2021;296:100394.
33. Tóth E, Varga É, Kulcsár PI, Kocsis-Jutka V, Krausz SL, Nyeste A. Improved LbCas12a variants with altered PAM specificities further broaden the genome targeting range of Cas12a nucleases. Nucleic Acids Res. 2020;48(7):3722–33.
34. Sasamoto NK, Elias KM. Early detection of ovarian cancer, cold spring harb. Perspect Med. 2023;13(11):a041337.
35. Paul B, Montoya G. CRISPR-Cas12a: Functional overview and applications. Biomed J. 2020;43(1):8–17.
36. Rananaware SR, Vesco EK, Shoemaker GM, Anekar SS, Sandoval LSW, Meister KS, Macaluso NC, Nguyen LT, Jain PK. Programmable RNA detection with CRISPR-Cas12a. Nat Commun. 2024;14(1):5409–23.
37. Wang Y, Li JQ, Li SJ, Zhu X, Wang XX, Huang JF, et al. LAMP-CRISPR-Cas12-based diagnostic platform for detection of Mycobacterium tuberculosis complex using real-time fluorescence or lateral flow test. Microchim Acta. 2021;188(10):347.
38. Zhou SY, Dong JB, Deng LY, Wang GX, Yang M, Wang YZ, et al. Endonuclease-Assisted PAM-free Recombinase Polymerase Amplification Coupling with CRISPR/Cas12a (E-PfRPA/Cas) for Sensitive Detection of DNA Methylation. ACS Sensors. 2022;7(10):3032–40.
39. Wu YQ, Yuan QC, Zhu YF, Gao X, Song JB, Yin ZR. Improving FnCas12a Genome Editing by Exonuclease Fusion. The CRISPR Journal. 2020;3(6):503–11.

Publisher's Note